

Asymmetric Explosion of Type Ia Supernovae as Seen from Near Infrared Observations¹

Kentaro Motohara², Keiichi Maeda³, Christopher L. Gerardy⁴, Ken'ichi Nomoto⁵, Masaomi Tanaka⁵, Nozomu Tominaga⁵, Takuya Ohkubo⁵, Paolo A. Mazzali^{6,7,5}, Robert A. Fesen⁸, Peter Höflich⁹, and J. Craig Wheeler⁹

ABSTRACT

We present near-infrared spectra of late phase ($> 200^d$) Type Ia supernovae (SNe Ia) taken at the Subaru telescope. The [Fe II] line of SN 2003hv shows a clear flat-topped feature, while that of SN 2005W show less prominent flatness. In addition, a large shift in their line center, varying from -3000 to 1000 (km s^{-1}) with respect to the host galaxies, is seen. Such a shift suggests the occurrence of an off-center, non-spherical explosion in the central region, and provides important, new constraints on the explosion models of SNe Ia.

Subject headings: infrared: stars — supernovae: general — supernovae: individual (SN 2003du, SN 2003hv, SN 2005W)

Accepted for publication in the *Astrophysical Journal (Letters)*

1. Introduction and Summary

The brightness and approximate uniformity of Type Ia supernovae (SNe Ia) enable us to use them as reliable and distant standard candles, and provided evidence for the accelerating uni-

verse (Riess et al. 1998; Perlmutter et al. 1999). For precision cosmology, it is critical to understand the origin of diversity, as well as the explosion mechanism of SNe Ia that is still open to debate (see, e.g., Hillebrandt & Niemeyer 2000, for a review). Possible sources of diversity include the asymmetry of the explosion (Wang et al. 2003) due to the rotation of the progenitor white dwarfs (WDs) (Piersanti et al. 2003; Saio & Nomoto 2004; Uenishi, Nomoto & Hachisu 2003; Yoon & Langer 2003) and/or turbulent behavior of the deflagration flame (e.g., Gamezo et al. 2003; Röpke et al. 2006). Therefore, it is important to observationally investigate the distribution of the synthesized elements and the kinematical structure of the ejecta in order to constrain the explosion models.

In this respect, late-phase (~ 1 yr since the explosion) spectroscopy at near-infrared (NIR) wavelength provides important diagnostics. Because the ejecta become optically thin in late phases, spectroscopy provides an unbiased, direct view of the innermost regions. Well isolated [Fe II] emission lines at 1.257 and 1.644 μm enable us to trace the distribution of the most important

¹Based on data collected at Subaru Telescope, which is operated by the National Astronomical Observatory of Japan.

²Institute of Astronomy, University of Tokyo, Mitaka, Tokyo 181-0015, Japan; kmotohara@ioa.s.u-tokyo.ac.jp

³Department of Earth Science and Astronomy, Graduate School of Arts and Science, University of Tokyo, Meguro-ku, Tokyo 153-8902, Japan

⁴Astrophysics Group, Imperial College, Blackett Laboratory, Prince Consort Road, London SW7 2BZ, UK

⁵Department of Astronomy, University of Tokyo, Bunkyo-ku, Tokyo 113-0033, Japan

⁶Max-Planck-Institut für Astrophysik, Karl-Schwarzschild-Straße 1, 85741 Garching, Germany

⁷Instituto Nazionale di Astrofisica (INAF)-Osservatorio Astronomico di Trieste, Via Tiepolo 11, I-34131 Trieste, Italy

⁸Department of Physics and Astronomy, 6127 Wilder Laboratory, Dartmouth College, Hanover, NH 03755

⁹McDonald Observatory, University of Texas, Austin, TX 78712

isotopes synthesized in SNe Ia, i.e., ^{56}Ni (which decays into ^{56}Co and then ^{56}Fe) and other iron isotopes such as ^{54}Fe . NIR observations of the type Ia SN 1991T show a strongly peaked [Fe II] 1.644 μm line which appears symmetric with respect to the rest-frame of the host galaxy (Spyromilio et al. 1992; Bowers et al. 1997). The NIR [Fe II] line profile of SN 1998bu observed by Spyromilio et al. (2004) appears to have a somewhat less centrally-peaked emission profile.

This approach was highlighted by the discovery of a flat-topped [Fe II] 1.644 μm emission line in SN 2003du (Höflich et al. 2004). Such a line profile requires a central hole in the kinematic distribution of the radioactive ejecta. This sort of hollow radioactivity distribution is predicted in 1D explosion models (e.g., Nomoto et al. 1994, for a review) in which the innermost regions are burned under high densities, $\rho > 10^9 \text{g cm}^{-3}$, and electron capture produces stable isotopes of ^{58}Ni , ^{54}Fe , and ^{56}Fe , rather than radioactive ^{56}Ni . However, such a distribution is contrary to the predictions of state-of-the-art 3D deflagration simulations which predict large-scale turbulent mixing in the inner layers, and thus do not confine ^{56}Ni outside the central core. The Höflich et al. (2004) NIR spectrum of SN 2003du also indicate that the [Fe II] 1.257, 1.644 μm emission lines show a blueshift of 500–1,000 km s^{-1} with respect to the host galaxy.

However, since the observed sample size of late-phase NIR spectra is so small, it is not clear whether the flat-topped and blue-shifted lines are general properties of SNe Ia. Such observations are extremely difficult because even relatively nearby and bright SNe Ia are faint in NIR at late phases (e.g., $H = 20 \sim 21$ for SN 2003du at ~ 1 year after the explosion). We therefore have conducted NIR observations of SNe Ia using the Subaru with OH airglow suppressor (Table 1) and obtained 2 more late-phase 1–2 μm spectra of SN 2003hv and 2005W.

Detailed explanation and discussion of the spectra will be presented elsewhere (Motohara et al., in prep.). We briefly report two interesting results in this letter. (1) The [Fe II] lines of SN 2003hv also show a clear flat-topped feature. (2) The [Fe II] lines of SN 2005W show less prominent flatness. (3) A large velocity shift of the line center, varying from -3000 to 1000 (km s^{-1}) with respect to the host galaxies, exists.

Considering the uniformity in optical bands around the peak luminosity, the existence of such inhomogeneity and asymmetry in SNe Ia is surprising, and provides important, new constraints on the explosion models.

2. Observations

2.1. SN 2003du

SN 2003du was discovered by LOTOSS on 2003 Apr. 22.4 in UGC 9391 at about 15.9mag (Schwartz & Holvorcem 2003). It was confirmed to be a SN Ia by Kotak et al. (2003) who reported that the optical spectrum resembles that of SN 2002bo about 2 weeks before maximum, and reached maximum light in the B -band ($t_{B\text{max}} = 0^{\text{d}}$) on 2003 May 6.3 UT (JD 2452766.3 \pm 0.5) (Anupama, Sahu, & Jose 2005).

As reported Höflich et al. (2004), JH -band spectroscopy of SN 2003du was carried out using OHS/CISCO (Iwamuro et al. 2001; Motohara et al. 2002) at Subaru. For this work, we re-reduced the data taken on 2004 Feb 27.5 (+297^d), which were processed in a standard procedure of flat fielding, sky subtraction, bad-pixel correction, and residual sky subtraction. The flux was scaled using the H -band photometry that was taken on 2004 April 2.5, assuming that the change in the brightness is negligible at the late phase. Wavelength was calibrated using the standard pixel-wavelength relation of CISCO, of which the systematic error is estimated to be less than 0.5 pixels ($< 3\text{\AA}$).

2.2. SN 2003hv

SN 2003hv was discovered by LOTOSS on 2003 Sep. 9.5 (UT) in NGC 1201 at about 12.5mag (Beutler & Li 2003), and confirmed to be a SN Ia by the spectrum taken on 2003 Sep. 10.4 which resembles that of SN 1994D two days after maximum (Dressler et al. 2003). We therefore assume maximum light in the B -band to be JD2452891.

Our JH -band spectroscopy of SN 2003hv was carried out using OHS/CISCO on 2004 Oct 6 (epoch +394^d). The JH -band spectroscopy consists of 6 frames of 2000 sec exposure with an $0''.5$ slit, providing a wavelength resolution of ~ 400 . The A2 star SAO 169939 was observed after the target to correct the atmospheric and instrumental absorption pattern. The data were reduced in

the same manner as that of SN 2003du.

2.3. SN2005W

SN 2005W was discovered on 2005 Feb. 1.4 (UT) in NGC 691 at about 15.2mag (Nakano & Li 2005), and confirmed to be a SN Ia about a week before maximum on 2005 Feb 2.7 (UT) (Elias-Rosa et al. 2005). The expansion velocity is measured to be $\sim 11600 \text{ km s}^{-1}$ from the Si II line. We assume maximum light in the *B*-band to be 2005 Feb 10 (JD 2453413).

Our *JH*-band spectroscopy of SN 2005W was carried out on 2005 Sep 12 (epoch +214^d) by OHS/CISCO. It consists of 4 frames of 1000 sec exposure with an 0".5 slit. The A2 star HIP 20091 was observed after the target to correct the atmospheric and instrumental absorption pattern. The data were reduced in the same manner as that of SN 2003du.

3. Results

The NIR spectra are shown in Figure 1. It can be seen that all the observed SNe Ia exhibit strong [Fe II] 1.257 μm and 1.644 μm lines. We discovered two important features.

First, the line center of [Fe II], corrected for the redshift of the host galaxies, is not identical for the three events. With respect to the rest wavelength of the line (1.644 μm), 2 SNe Ia (2003du, 2003hv) show a blueshift, while the other SN (2005W) shows a redshift. The corresponding velocity shifts relative to the hosts' rest frame are -2600 km s^{-1} , -2100 km s^{-1} , and $+1400 \text{ km s}^{-1}$, for SNe 2003hv, 2003du, and 2005W, respectively.

Such a velocity shift is confirmed by a mid-infrared(MIR) spectrum of SN 2003hv taken by the IRS/Spitzer Space Telescope at $\sim +360^{\text{d}}$ after maximum brightness (Fig. 2; Gerardy et al., in prep.). One of the strongest emission features is identified as the ground-state fine-structure line of [Co III] at 11.89 μm ($a^4\text{F}_{9/2} - a^4\text{F}_{7/2}$). The well-isolated [Co III] line also shows a velocity shift which is consistent with that seen in the NIR [Fe II] 1.644 μm line, to within the noise level of the MIR feature.

Secondly, we find that the observed [Fe II] lines show a large variety in their shape (Figure 1). The spectrum of SN 2003hv clearly shows a flat-topped boxy profile like that seen at much lower

S/N in SN 2003du. Indeed, the higher *S/N* of the SN 2003hv spectrum places a much stronger constraint on the flatness of the core of the [Fe II] line. In contrast, the [Fe II] line profile of SN 2005W shows no evidence of a central flat top.

The boxy profile of [Fe II] lines seen in SN 2003du and SN 2003hv suggests the absence of radioactive ^{56}Ni below $\sim 3000 \text{ km s}^{-1}$ (measured from the center of the ^{56}Ni distribution). We note that the observed epoch of SN 2003hv is more advanced than SN 2003du. At a later epoch, the line profile should follow the ^{56}Ni distribution more closely (§4). Effects of possible line deformation due to electron and line scatterings will also effectively vanish. The present result of SN 2003hv confirms the existence of the ^{56}Ni -empty hole more strongly than that of SN 2003du.

4. Discussion

In this section we discuss the impact of our findings for understanding the explosion mechanism. It is widely agreed that the explosion of a SN Ia starts from a deflagration (Nomoto, Sugimoto, & Neo 1976). In the spherical deflagration models, electron capture leads to the synthesis of ^{58}Ni , ^{54}Fe , and ^{56}Fe (not via ^{56}Ni decay), thus creating an almost ^{56}Ni -empty hole (e.g., Nomoto, Thielemann, & Yokoi 1984). In multi-D models, the ignition of the deflagration may be off-center, producing a non-spherical burning region (Wunsch & Woosley 2004; Plewa, Calder, & Lamb 2004). In some cases, the deflagration to detonation transition (DDT) may occur (delayed detonation models: Khokhlov 1991). The DDT may also take place non-spherically (Livne 1999) even if the deflagration does not have bulk kinematical offset.

The flat-topped [Fe II] NIR lines in SNe 2003hv and 2003du indicate that the highest density region occupied by neutron-rich Fe-peak isotopes is not mixed with the surrounding region where the dominant isotope is ^{56}Ni (Höflich et al. 2004). Figure 2 shows a spectrum for the spherical deflagration explosion model W7 (Nomoto et al. 1984) at 400^d since the explosion, compared with that of SN 2003hv. This is calculated by solving transport of γ -rays produced in the decay chain $^{56}\text{Ni} \rightarrow ^{56}\text{Co} \rightarrow ^{56}\text{Fe}$ and iteratively solving NLTE rate equations (Mazzali et al. 2001; Maeda et al. 2006). Positrons produced by the ^{56}Co -decay are

assumed to be trapped on the spot, since the mean free path of positrons is expected to be small at this epoch (Milne et al. 2001).

The model shows that the flat-topped profile is consistent with the [Fe II] 1.644 μm emission for the reason as described above. The asymmetry in the profile, mildly peaking in the red, is due to the weak contributions of [Fe II] 1.664, 1.677 μm .

The shift of [Fe II] lines suggests that the distribution of ^{56}Ni (which decays to ^{56}Fe via ^{56}Co) produced at the explosion is asymmetric, showing the bulk kinematical offset of $\gtrsim 2000 \text{ km s}^{-1}$ with respect to the SN rest frame. This suggests that, unlike the spherical models, the carbon ignition may take place off-center. The flat-topped [Fe II] line profiles suggest that electron capture in the high density off-center deflagration region creates the neutron-rich hole as in 1D models, at least in SNe 2003du and 2003hv. The neutron-rich hole is offset along with the bulk ^{56}Ni distribution. This indicates that the highest density burning in these SNe took place quite far away from the center of the progenitor star.

The blueshifted and flat-topped profile of [Fe II] can also be reproduced by symmetric and opaque dusty core, like [O I] $\lambda\lambda 6300, 6364$ observed in late phase Type II SN (Elmhamdi et al. 2003). If this is the case in the present results, MIR [Co III] line, which will be far less affected by dust extinction, may show much smaller blueshift than NIR [Fe II]. However, the [Co III] line shows almost same blueshift as [Fe II] (Fig. 2). Therefore, it is unlikely that the flat-topped profile is caused by the opaque dust core.

Adding the result of SN 1991T (Spyromilio et al. 1992; Bowers et al. 1997), 2 SNe (SN 2003du, SN 2003hv) out of 4 SNe Ia show the boxy [Fe II] profile (Figure 1), while SN1991T and SN 2005W do not. This could indicate that the distribution of ^{56}Ni in the innermost region of the SN Ia explosion might differ from object to object. SNe Ia with a non-boxy line profile might experience more mixing than those with a boxy profile (e.g., SN 2003hv) in the innermost region. Another possibility is that the density of the progenitor where the ignition takes place differs from object to object, and SN Ia with the peaked [Fe II] explodes at a low density so as not to produce electron capture isotopes.

Alternatively, the different line shape could be due to an age effect, i.e., due to a variation in the extent to which the energy deposition from the radioactivity is kept local. At earlier epochs, γ -rays are the dominant heating source. Since the γ -ray penetration is not a local process, the innermost region, even without ^{56}Ni there, can be heated effectively. At later epochs, contribution from the local positron energy input becomes larger, and the line profile should follow the ^{56}Ni distribution more closely. Therefore, we expect that the line shape could evolve from a peaked to a flat-topped profile. This may partially explain the fact that the most aged SN Ia 2003hv shows the clean flat-topped boxy [Fe II] line. Indeed, this provides an observational test of our model.

We suggest a future test to estimate the age effect and confirm our interpretation of the ^{56}Ni : a temporal series of NIR nebular spectra for an individual SN Ia. The shape of [Fe II] line is expected to start getting flat at $\sim 250^{\text{d}}$, and may become totally flat at $\sim 500^{\text{d}}$. Thereafter, it may start showing a peaked profile at $\sim 1,000^{\text{d}}$ again, depending on the amount of positrons that can escape the ejecta (Milne et al. 2001). Also, spectra at different wavelengths from optical to the MIR will be useful to investigate the distribution of different ions and heating radioactive isotopes (e.g., Figure 2). Because the line profiles from different ions and from different energy levels are dependent on the ionization and thermal structure of the ejecta, further detailed theoretical study is necessary to make use of these observations efficiently.

We thank all the staff at the Subaru observatory for their excellent support of the observations. This work has been supported in part by the Grant-in-Aid for Scientific Research (17030005, 17033002, 18104003, 18540231) and the 21st Century COE Program (QUEST) from the JSPS and MEXT of Japan. CLG is supported through UK PPARC grant PPA/G/S/2003/00040. JCW is supported by NSF Grant AST-0406740.

REFERENCES

- Anupama, G. C., Sahu, D. K., & Jose, J. 2005, *A&A*, 429, 667
- Beutler, B. & Li, W. 2003, *IAU Circ.*8197
- Bowers, E. J. C., et al. 1997, *MNRAS*, 290, 663
- Dressler, A., Phillips, M., Morrell, N., & Hamuy, M. 2003, *IAU Circ.*, 8198
- Elias-Rosa, N., Navasardyan, H., Harutunyan, A., Benetti, S., Turatto, M., Pastorello, A., & Patat, F. 2005, *IAU Circ.*, 8479
- Elmhamdi, A., et al. 2003, *MNRAS*, 338, 939
- Gamezo, V. N., Khokhlov, A. M., Oran, E. S., Chtchelkanova, A. Y., & Rosenberg, R. O. 2003, *Science*, 299, 77
- Hillebrandt, W., & Niemeyer, J. C. 2000, *ARA&A*, 38, 191
- Höflich, P., Gerardy, C. L., Nomoto, K., Motohara, K., Fesen, R. A., Maeda, K., Ohkubo, T., & Tominaga, N. 2004, *ApJ*, 617, 1258
- Iwamuro, F., Motohara, K., Maihara, T., Hata, R., & Harashima, T. 2001, *PASJ*, 53, 335
- Khokhlov, A.M. 1991, *A&A*, 245, 114
- Kotak, R., Meikle, W. P. S., & Rodriuez-Gil, P. 2003, *IAU Circ.*, 8122
- Livne, E. 1999, *ApJ*, 527, L97
- Maeda, K., Nomoto, K., Mazzali, P.A., & Deng, J. 2006, *ApJ*, 640, 854
- Mazzali, P. A., Nomoto, K., Patat, F., & Maeda, K. 2001, *ApJ*, 559, 1047
- Milne, P. A., The, L. -S., & Leising, M. D. 2001, *ApJ*, 559, 1019
- Motohara, K., et al., T. 2002, *PASJ*, 54, 315
- Nakano, S. & Li, W. 2005, *IAU Circ.*, 8475
- Nomoto, K., Sugimoto, D., & Neo, S. 1976, *Ap&SS*, 39, L37
- Nomoto, K., Thielemann, F. -K., & Yokoi, K. 1984, *ApJ*, 286, 644
- Nomoto, K., Yamaoka, H., Shigeyama, T., Kumagai, S., & Tsujimoto, T. 1994, in *Supernovae, Les Houches Session LIV*, ed. S.A. Bludman et al. (Amsterdam: North-Holland), 199
- Perlmutter, S., et al. 1999, *ApJ*, 517, 565
- Piersanti, L., Gagliardi, S., Iben, I., Jr., & Tornambé, A. 2003a, *ApJ*, 583, 885
- Plewa, T., Calder, A. C., & Lamb, D. Q. 2004, *ApJ*, 612, L37
- Riess, A. G., et al. 1998, *AJ*, 116, 1009
- Röpke, F. K., Gieseler, M., Reinecke, M., Travaglio, C., & Hillebrandt, W. 2006, *A&A*, 453, 203
- Saio, H., & Nomoto, K. 2004, *ApJ*, 615, 444
- Schwartz, M., & Holvorcem, P. R. 2003, *IAU Circ.*, 8121
- Spyromilio, J., Meikle, W. P. S., Allen, D. A., & Graham, J. R. 1992, *MNRAS*, 258, 53
- Spyromilio, J., Gilmozzi, R., Sollerman, J., Leibundgut, B., Fransson, C., & Cuby, J-G. 2004, *A&A*, 426, 547
- Uenishi, T., Nomoto, K., & Hachisu, I. 2003, *ApJ*, 595, 1094
- Wang, L., et al. 2003, *ApJ*, 591, 1110
- Wunsch, S., & Woosley, S. E. 2004, *ApJ*, 616, 1102
- Yoon, S. -C., & Langer, N. 2003, *A&A*, 312, L53

TABLE 1
 INFRARED SPECTROSCOPY OBSERVING LOG

| Name | Host | z_{Host} | Obs. Date (UT) | Epoch ^a (d) | $\lambda\lambda(\text{\AA})$ | $\lambda/\Delta\lambda$ | Exposure (s) | Slit (") |
|--------|----------|-------------------|----------------|------------------------|------------------------------|-------------------------|--------------|----------|
| 2003du | UGC 9391 | 0.006384 | 2004 Feb 27.5 | +297.2 | 11080–18040 | 400 | 4000 | 0.5 |
| 2003hv | NGC 1201 | 0.005604 | 2004 Oct 06.5 | +394 | 11080–18040 | 400 | 12000 | 0.5 |
| 2005W | NGC 691 | 0.008889 | 2005 Sep 12.6 | +214 | 11080–18040 | 400 | 4000 | 0.5 |

^aEpochs are with respect to the epoch of B -band maximum light ($t_{B\text{max}} = 0$).

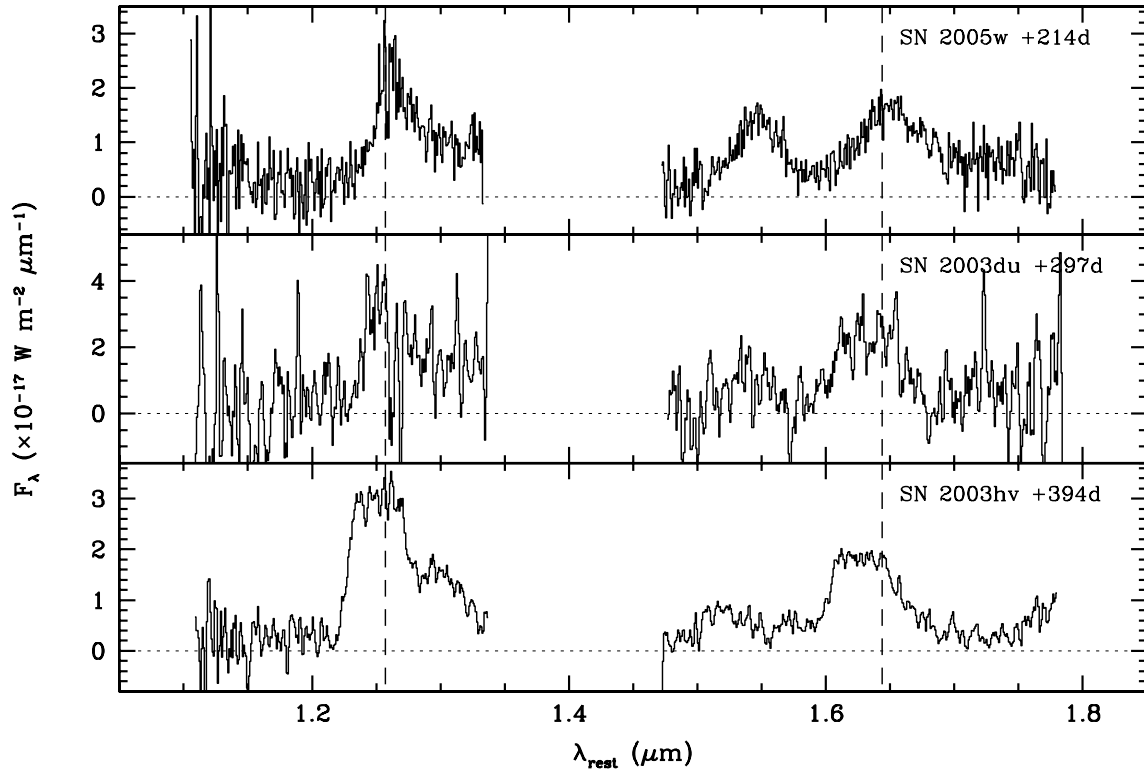


Fig. 1.— NIR 1 – 2 μm spectra of late-phase SNe Ia, converted to the rest wavelength at the host galaxies. All the spectra are smoothed with 3 pixel boxcar filter. Vertical dashed lines show the position of [Fe II] 1.257 μm and 1.644 μm lines.

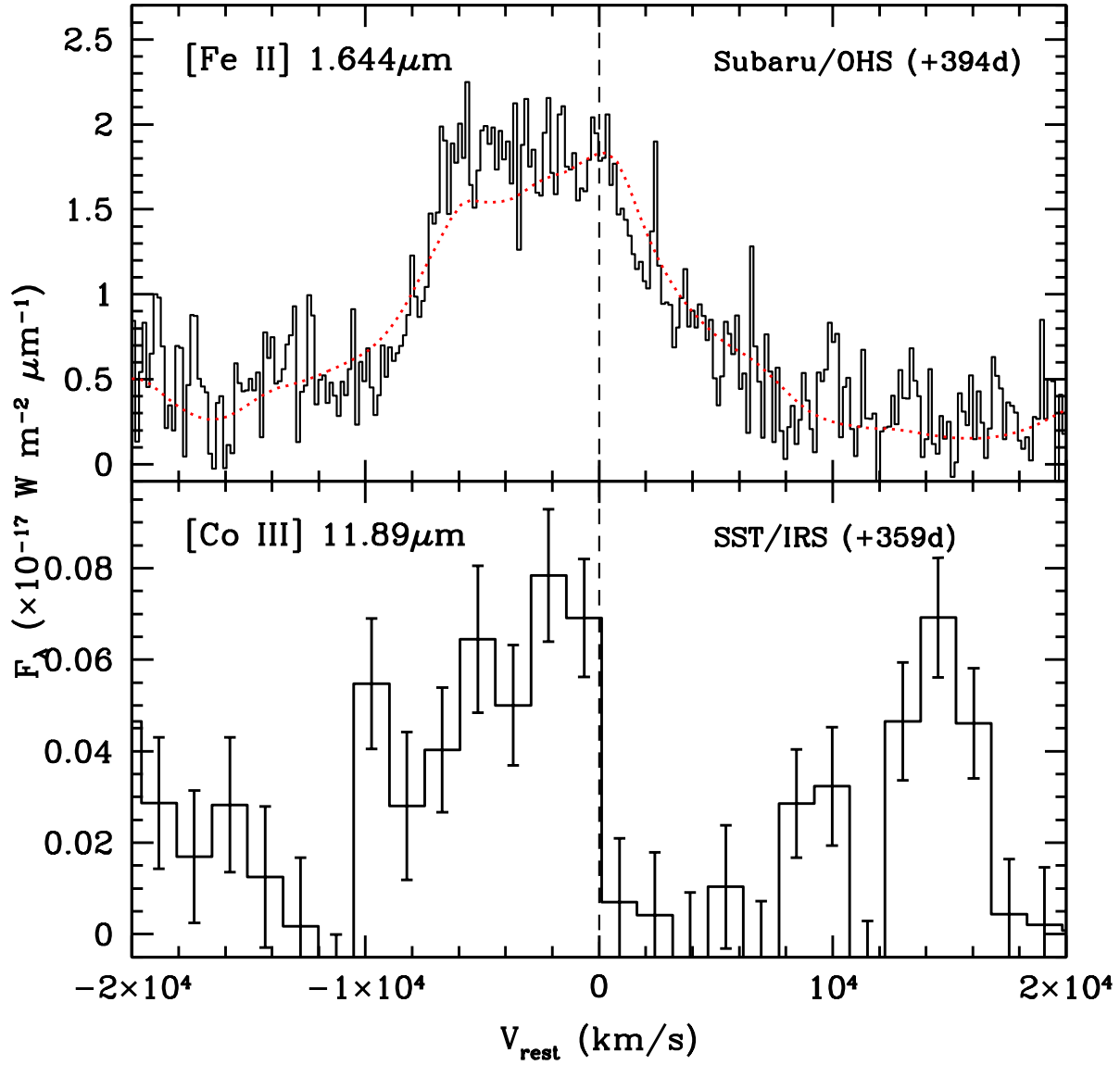


Fig. 2.— [Fe II] 1.644 μm (top) and [Co III] 11.89 μm (bottom) emission lines of SN 2003hv (solid). Overlapped with the [Fe II] line is the 1D explosion model W7 at 400^d since the explosion (dotted). The model flux is arbitrarily scaled to fit the observed flux, as well as shifted to the blue by 2600 km s^{-1} .